

Calibrated and Efficient Sampling-Free Confidence Estimation for LiDAR Scene Semantic Segmentation

Hanieh Shojaei Miandashti

Qianqian Zou

Claus Brenner

Institute of Cartography and Geoinformatics, Leibniz University Hannover
Appelstraße 9a, Hannover, 30167, Germany

hanieh.shojaei@ikg.uni-hannover.de

qianqian.zou@ikg.uni-hannover.de

claus.brenner@ikg.uni-hannover.de

Abstract

Reliable deep learning models require not only accurate predictions but also well-calibrated confidence estimates to ensure dependable uncertainty estimation. This is crucial in safety-critical applications like autonomous driving, which depend on rapid and precise semantic segmentation of LiDAR point clouds for real-time 3D scene understanding. In this work, we introduce a sampling-free approach for estimating well-calibrated confidence values for classification tasks, achieving alignment with true classification accuracy and significantly reducing inference time compared to sampling-based methods. Our evaluation using the Adaptive Calibration Error (ACE) metric for LiDAR semantic segmentation shows that our approach maintains well-calibrated confidence values while achieving increased processing speed compared to a sampling baseline. Additionally, reliability diagrams reveal that our method produces underconfidence rather than overconfident predictions, an advantage for safety-critical applications. Our sampling-free approach offers well-calibrated and time-efficient predictions for LiDAR scene semantic segmentation.

crucial; it ensures that the confidence values truly represent the actual probability of correctness, enabling users to better understand and trust the model’s outputs.

Confidence calibration must address both aleatoric uncertainty, which arises from irreducible inherent noise in the data, and epistemic uncertainty, which stems from the uncertainty in the model’s parameters and can diminish with additional data [4]. Effectively considering the impact of both aleatoric and epistemic uncertainties on confidence computation leads to better-calibrated confidence estimates.

Bayesian deep learning provides a principled approach for uncertainty modeling by integrating probabilistic methods into deep learning frameworks, rather than using point estimates [9]. To capture epistemic uncertainty in a neural network, Bayesian Neural Networks (BNNs) place a prior distribution over the model’s weights and compute a posterior distribution over these weights using Bayesian inference [8, 15]. Since exact inference is intractable, methods like deep ensembles [11] approximate this posterior, estimating epistemic uncertainty by computing the variance of the outputs of different model configurations.

Regarding aleatoric uncertainty, the logit-sampling method [8] directly incorporates the estimation of this uncertainty into the training process by modeling logits as Gaussian distributions and sampling from these during training [8]. This approach necessitates sampling during inference as well; increasing the number of samples improves confidence accuracy but also increases inference time.

The primary contribution of this work is the development of a novel confidence estimation method that obviates the need for Monte Carlo sampling while still maintaining well-calibrated confidence values, capturing both aleatoric and epistemic uncertainties in a semantic segmentation task, as follows.

During inference, each input results in one predicted Gaussian distribution per class, each given by its mean

1. Introduction

The confidence value in deep learning quantifies the predicted probability that a model assigns to its chosen output class. Although intended to reflect the model’s certainty about its predictions, deep learning models often fail to capture the inherent uncertainty in the outputs, resulting in overconfident predictions [5]. This issue is particularly critical in applications requiring precise model reliability, where poor uncertainty representation can lead to dangerously misleading confidence scores, especially when predictions are incorrect. Proper calibration of these scores is

and standard deviation. As in the case of standard, point-estimate networks, the class with the largest mean is selected as the winner class. Clearly, if the mean of this winner class is larger than the mean of any competing class by a large margin (where ‘large’ must be understood in relation to the involved standard deviations), we would be highly confident about our decision. More precisely, we define confidence as the probability that our selection of the winner class is correct, given all class distributions. Equivalently, this is the probability that a value drawn from the winner class distribution is larger than any value drawn from any of the other distributions. While details can be found in Sec. 3.2, we note here that this probability can be easily computed in closed-form for the case of two classes, can be approximated via Monte Carlo simulation for more than two classes, and in addition, a closed-form and thus, sampling-free solution for a lower (i.e., safe) bound can be given, which we have found to be quite tight in practice.

Furthermore, to account for epistemic uncertainty, we average confidence values across an ensemble of models. This method yields a robust semantic segmentation map for a LiDAR scene with well-calibrated confidence values.

In summary, we make two key claims. **First**, our sampling-free approach generates confidence values that closely approximate true confidence levels, effectively calibrated against the actual classification accuracy. This alignment is evidenced by our performance on the Adaptive Calibration Error (ACE) [16] metric and further observed in the reliability diagram [5]. Additionally, our method produces underconfident rather than overconfident values, making it particularly valuable for safety-critical decision-making. **Second**, our proposed sampling-free approach reduces significantly inference time compared to sampling methods such as logit-sampling while maintaining calibration accuracy.

2. Related works

2.1. Confidence calibration

Previous research on confidence calibration of deep learning models typically falls into two categories. The first involves post-processing techniques that adjust classifier outputs without retraining the model [5, 10, 20]. Temperature Scaling [5] exemplifies this by recalibrating model logits using a single parameter optimized on a validation set. Extending this approach, Logistic Scaling [5] and Dirichlet Scaling [10] employ logistic regression transformations and Dirichlet distributions, respectively.

Post-processing techniques primarily focus on aligning the predicted probabilities with the actual likelihood of outcomes. However, these methods do not fundamentally alter the underlying model or its uncertainties that contribute to initial miscalibrations. They modify the output to appear

more accurate in terms of confidence but do not resolve the root causes of why the model might be uncertain or prone to errors in the first place. Thus, while effective for calibration, they do not address deeper model uncertainties or biases. Additionally, temperature scaling faces computational inefficiencies due to multiple validation data passes required for parameter optimization.

In contrast, the second category incorporates uncertainty directly into the training phase, enhancing models’ inherent ability to account for data variability.

2.2. Uncertainty estimation in classification tasks

Methods such as Bayesian neural networks [15] and evidential deep learning [18] equip models to inherently represent uncertainty, providing a more fundamental solution to confidence calibration challenges. Several methods for estimating epistemic uncertainty have emerged in recent years, primarily based on Bayesian neural networks [9]. These methods enable models to approximate the true posterior distribution, improving their ability to capture uncertainty [12]. Prominent examples include Deep Ensembles [11] and Monte Carlo Dropout [3], which estimate epistemic uncertainty by computing the variance over multiple classification outputs during inference. However, while deep ensemble models effectively indicate model confidence by averaging softmax outputs from multiple models, they may still require further calibration to align the softmax probabilities with actual outcome probabilities.

To accurately calibrate softmax outputs by accounting for the underlying true distribution, the logit-sampling approach proposes a method that assumes a Gaussian distribution for the logits of each class [8]. This method involves directly estimating the parameters of these Gaussian distributions during training, which then allows for a more refined and statistically grounded calibration of the softmax probabilities. During inference, calibrated confidence is computed by averaging the softmax values from Monte Carlo samplings across each distribution.

2.3. Semantic segmentation of LiDAR point clouds

There are two primary approaches for deep learning-based semantic segmentation of 3D LiDAR data, as described in [6]: point-wise networks that process 3D input data, such as 3D voxels [7] or unordered point clouds [17], and projection-based methods that convert 3D point clouds into 2D input data using range-view image representations [2, 19]. Projection-based methods, utilizing the established strengths of 2D convolutional neural networks in image processing tasks, achieve higher accuracy and faster processing speeds compared to point-wise networks, as demonstrated in [2]. SalsaNext [2] used Monte Carlo Dropout to estimate epistemic uncertainty based on the variance of the multiple outputs. Although Monte Carlo dropout can incorporate un-

certainty in the segmentation model, deep ensembles have shown superior performance for epistemic uncertainty over Monte Carlo Dropout in recent years [13].

In our present work, we employ deep ensembles to compute the epistemic uncertainty. Additionally, we utilize the logit-sampling approach for modeling Gaussian distributions over the network outputs, enabling the precise computation of our proposed confidence value considering aleatoric uncertainty.

3. Methodology

Our approach builds on the logit-sampling method to predict Gaussian distributions over the outputs of a classification model. Considering the class with the highest mean as the predicted class, we directly compute its well-calibrated confidence value by evaluating the probability that logit scores from this class exceed those of competing classes, thus efficiently capturing aleatoric uncertainty without the need for sampling from Gaussian distributions. Additionally, we employ a deep ensemble strategy to account for the model uncertainty in computing the confidence value. This approach aggregates confidence evaluations from a collection of models, thereby enhancing the robustness and reliability of our confidence predictions.

Firstly, we provide a brief introduction in Sec. 3.1 regarding the model used for predicting the probabilistic distributions of logits, which encodes aleatoric uncertainty in the outputs. Secondly, our proposed confidence computation is explained in Sec. 3.2, which is calibrated and based on the outputs of such model. Consequently, the total uncertainty score for each pixel is derived from the predicted confidence values as $1 - \textit{confidence}$.

3.1. Predicting Gaussian distributions over the outputs

The idea of directly predicting Gaussian distributions over the outputs of a neural network, in the logit space, was originally introduced by the logit-sampling approach [8]. This approach assumes that outputs in the logit space, before going through a softmax function, are corrupted by Gaussian noise. This logit noise affects the model’s confidence in selecting a certain class as the output label. In this setup, confidence is not represented as a point estimate; instead, a distribution is modeled over the confidence of each class for a given pixel. By sampling from each Gaussian distribution, a range of logit scores are passed to the softmax function to compute the probability vectors. Consequently, the loss function is calculated based on the average of the softmax results from the sampled logits, rather than from a single logit score, as shown in Eq. (1).

$$L_x = - \sum_i \log \left(\frac{1}{T} \sum_t \text{softmax}(\hat{\mathbf{x}}_{i,t}) \right) \quad (1)$$

$$\hat{\mathbf{x}}_{i,t} = \boldsymbol{\mu}_i + \text{diag}(\boldsymbol{\sigma}_i)\boldsymbol{\epsilon}_t, \quad \boldsymbol{\epsilon}_t \sim \mathcal{N}(0, \mathbf{I}) \quad (2)$$

This loss function allows the model to consider T samples from the joint distribution of the scores over C classes. In Eq. (1), $\hat{\mathbf{x}}_{i,t}$ denotes the t -th logit sample vector for C classes at the i -th pixel, which is computed based on the predicted mean vector $\boldsymbol{\mu}_i$ and variance vector $\boldsymbol{\sigma}_i^2$ as described in Eq. (2). $\boldsymbol{\mu}_i$ and $\boldsymbol{\sigma}_i^2$ parameterize C Gaussian distributions in logit space, as the model outputs.

3.2. Confidence computation

3.2.1. Exact and approximate computation

The proposed method is based on the Gaussian distributions over the logits. As usual, one would predict the class whose predicted mean is maximal. Let there be C classes, for each of which a Gaussian distribution $\mathcal{N}(\cdot|\mu_i, \sigma_i^2)$, $1 \leq i \leq C$ is predicted. Then, without loss of generality, we may assume $\mu_1 \geq \mu_i$ for $i \geq 2$, so that class 1 is selected as the predicted class. The confidence is then defined as the probability that this selection is correct, which, given random variables $X_i \sim \mathcal{N}(\cdot|\mu_i, \sigma_i^2)$, is $P(X_1 \geq \{X_i\}_{i \geq 2})$, equivalent to $P(X_1 \geq \max_{i \geq 2} X_i)$.

As there is no closed-form solution to compute this probability in the general case, it may be approximated by computing a relative frequency by simulation. Similar to the training phase, C samples X_i , $1 \leq i \leq C$ are drawn (one from each Gaussian), and it is determined if X_1 is largest. From repeating this experiment N times, the relative frequency of cases $X_1 \geq \max_{i \geq 2} X_i$ is computed. This method requires NC draws.

It is easily seen that the required probability is given by

$$P(X_1 \geq \max_{i \geq 2} X_i) = \int_{-\infty}^{+\infty} \varphi_1(x) \prod_{i=2}^C \Phi_i(x) dx, \quad (3)$$

where we have used $\varphi_i(x) = \mathcal{N}(x|\mu_i, \sigma_i^2)$ for the Gaussian densities and $\Phi_i(x)$ for their associated cumulative distribution functions. This integral can be approximated via Monte Carlo simulation using

$$P(X_1 \geq \max_{i \geq 2} X_i) \approx \frac{1}{N} \sum_{k=1}^N \prod_{i=2}^C \Phi_i(x_k), \quad (4)$$

with $x_k \sim \varphi_1$, requiring only N samples to be drawn (which in fact can be re-used by scaling and shifting a fixed set of samples).

3.2.2. Sampling-free confidence value quantification

For the special case of two classes, a closed-form solution can be given, because $P(X_1 \geq X_2) = P(Z \geq 0)$ with

$Z := X_1 - X_2$. As $Z \sim \mathcal{N}(\cdot | \mu_1 - \mu_2, \sigma_1^2 + \sigma_2^2)$ it follows that

$$P(X_1 \geq X_2) = \Phi(\mu_1 - \mu_2 | 0, \sigma_1^2 + \sigma_2^2) =: \Phi_{1,2}, \quad (5)$$

which unfortunately does not extend readily to $C > 2$ classes. However, using pairwise $\Phi_{1,i}$, $i \geq 2$, the following lower bound holds

$$P(X_1 \geq \max_{i \geq 2} X_i) \geq \prod_{i=2}^C \Phi_{1,i}, \quad (6)$$

which follows from the fact that the integral in Eq. (3) is the expected value $\mathbb{E}[\prod_{i=2}^C \Phi_i(X)]$ under the distribution $X \sim \varphi_1$, and since all $\Phi_i(x)$ are strictly monotonically increasing functions of x , their covariance is non-negative, from which it follows that $\mathbb{E}[\Phi_i(X)\Phi_j(X)] \geq \mathbb{E}[\Phi_i(X)]\mathbb{E}[\Phi_j(X)]$, yielding Eq. (6). (For products of more than two terms this follows by recursive application, noting that any product of Gaussian cumulative distribution functions is strictly monotonically increasing as well.)

To conclude, given the predicted class distributions, a lower bound for the confidence can be computed by simply evaluating $C - 1$ ‘pairwise’ cumulative distribution functions, requiring no sampling. To give some intuition, if class 1 is a clear winner, the confidence will be 1. If the winner class is challenged only by one alternative class, the lower bound Eq. (6) reduces to Eq. (5), and the bound is exact. If more than one other class challenges the winner class, the lower bound will underestimate the confidence. Experiments demonstrate that confidence values derived from the lower bound approach closely approximate those obtained through Monte Carlo integration (Eq. (4)), which suggests that the lower bound effectively estimates the true values.

4. Experiments

4.1. Experimental details

4.1.1. Model and dataset

We evaluate our proposed sampling-free confidence computation on LiDAR semantic segmentation using the SalsaNext [2] model applied to real-world 3D LiDAR scenes from the SemanticKITTI dataset [1]. Each 3D scan from SemanticKITTI was converted into a $[64 \times 1024 \times 5]$ spherical range-view image with channels for 3D point coordinates (x, y, z) , intensity, and range values, serving as input for segmentation into 20 object classes commonly found in urban scenes. We modified SalsaNext to predict Gaussian distributions in the outputs to incorporate aleatoric uncertainty. We used 150 samples in the logit space per forward pass during training, with the loss function defined in Eq. (1). Additionally, to capture epistemic uncertainty, we employed deep ensembles, training five independently initialized models to generate a diverse set of outputs.

4.1.2. Evaluation metrics

The classification performance of semantic segmentation models is commonly evaluated using the mean Intersection over Union (mIoU) metric, which accounts for the inherent class imbalance in semantic segmentation datasets and is well-suited for real-world applications.

To assess the calibration of the confidence values for predicted classes, we employ the ACE [16] alongside a reliability diagram [5]. In contrast to the Expected Calibration Error (ECE) [14], ACE assigns equal weight to each bin in the reliability diagram, defined as

$$\text{ACE} = \frac{1}{M} \sum_{m=1}^M |c_m - \text{Acc}_m|, \quad (7)$$

where M represents the number of non-empty bins, c_m is the average confidence within bin m , and Acc_m is the corresponding average accuracy.

4.2. Comparative analysis of sampling-based and sampling-free confidence computations

To support our first claim that the sampling-free lower bound approach closely estimates the true confidence values, we compare these confidence values with those obtained from the Monte Carlo integration. They are computed based on Eq. (6) and Eq. (4), respectively. The scatter plot in Fig. 1a illustrates this comparison on a subset of test samples, with x -axis representing the exact confidence values and the y -axis showing the lower bound estimation. The red dashed line denotes the ideal $y = x$ line, where the lower bound would match the exact computation.

Fig. 1a shows that the lower bound estimation predominantly aligns closely with or slightly underestimates the exact values, evidenced by the clustering of points below the $y = x$ line. This pattern indicates that the lower bound estimation tends to behave conservatively, often yielding slightly underestimated confidence values across a broad range.

Additionally, Fig. 1b contrasts the true classification accuracy (y -axis) with the exact confidence computation, the sampling-free lower bound approach and the logit-sampling baseline. Here, the sampling-free lower bound approach, depicted by the green line, consistently shows more conservative confidence estimates relative to the logit-sampling baseline and the exact values. This visualization underscores the differences in calibrated confidence between the methods, highlighting the conservative nature of our sampling-free approach.

Evaluated with real-world empirical data, the results indicate that under actual conditions, it is uncommon for many classes to have competitive logits compared to the true class. Consequently, our proposed sampling-free approach not only serves as a lower bound but also demon-

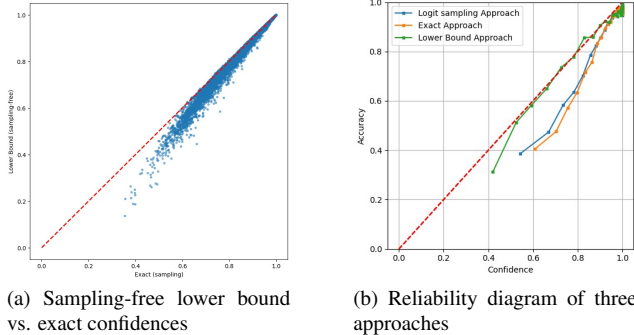


Figure 1. Comparative analysis of confidence estimation methods. Scatter plot (a) contrasts exact confidence values with those computed by the sampling-free lower bound approach. Reliability diagram (b) compares the calibration of confidence values between our sampling-free lower bound approach, exact values, and the logit-sampling method.

Table 1. Comparative analysis of inference time, mIoU, and ACE across various confidence calibration approaches.

Method	mIoU \uparrow	ACE (%) \downarrow	Inference Time (s) \downarrow
SalsaNext[2] (Uncalibrated)	52.06	6.81	0.12
SalsaNext[2]+DE[11]+Our sampling-free approach	51.60	3.30	0.28
SalsaNext[2]+DE[11]+Logit-sampling[8] (50 samples)	51.42	2.95	4.8
SalsaNext[2]+EDL[18]	48.30	5.32	0.12

strates a negligible difference from the exact value by the mean discrepancy of 0.0036.

4.3. Confidence calibration analysis

To validate our claims regarding the well-calibrated confidence values and the enhanced inference efficiency outlined in Sec. 1, we evaluated confidence values calculated by our sampling-free method against those derived from the uncalibrated SalsaNext, SalsaNext with logit-sampling conducted 50 Monte Carlo samplings during inference, and SalsaNext using Evidential Deep Learning (EDL). Tab. 1 provides a comparative analysis of the average inference time per scan and the calibration error across the test data for each method. Results indicate that the lowest confidence error is achieved with SalsaNext using our proposed approach and the logit-sampling approach. However, our method facilitates much faster inference and achieves a slight improvement in mIoU. In contrast, the uncalibrated Salsanext model yields slightly better mIoU results due to its fewer training parameters. Our training of Gaussian distributions doubles the parameters in the last layer.

The reliability diagrams in Fig. 2 illustrate the comparative calibration performance of our sampling-free approach. Generally, our method produces underconfident confidence estimations while logit-sampling exhibits overconfidence at confidence levels below 0.7. There is a minor decrease in the calibration of our proposed confidence values (0.35%) compared to those from the logit-sampling approach. How-

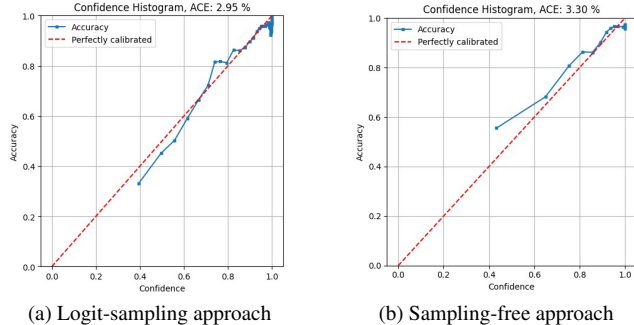


Figure 2. Reliability diagrams of the proposed sampling-free approach and the logit-sampling baseline. Both diagrams demonstrate the calibration of confidence values. Despite logit-sampling achieving a marginal calibration error improvement of 0.35%, it requires approximately 15 times longer to generate results.

ever, this slight trade-off is offset by the significant computational advantage of our method, as our method is 15.48 times faster than the logit-sampling approach. Furthermore, our approach tends to produce underconfident predictions, which is desirable in safety-critical applications and contributes to more reliable uncertainty quantification.

4.4. LiDAR semantic segmentation

In this section, we present a qualitative comparison between our proposed sampling-free approach prediction and those obtained from the logit-sampling by averaging softmax values across 50 Monte Carlo samples from the joint Gaussian distribution, as shown in Fig. 3. The performance of both methods demonstrates notable consistency. This is also evidenced by their mIoU values listed in Tab. 1, where our approach modestly surpasses logit-sampling by 0.18%. This illustrates that our proposed sampling-free method for confidence computation not only enhances the inference efficiency relative to the baseline logit-sampling approach but also provides accurate and well-calibrated predictions.

The overall uncertainty associated with the predicted class is depicted in Fig. 3f, with class outliers—unseen during training—shown in black. The uncertainty map uses a temperature scale to represent levels of uncertainty, with redder tones indicating higher uncertainty. The highest uncertainty is typically observed at class boundaries (e.g. between sidewalk and street), beneath vehicles, and around tree trunks, which present significant labeling challenges in point clouds, even manually. Additionally, areas far from the sensor also show increased uncertainty.

Our experiments demonstrate consistent confidence calibration across the test set, with qualitative results echoed in a different scan as shown in Fig. 4. A more complete quantitative and qualitative analyses are provided in the supplemental material.

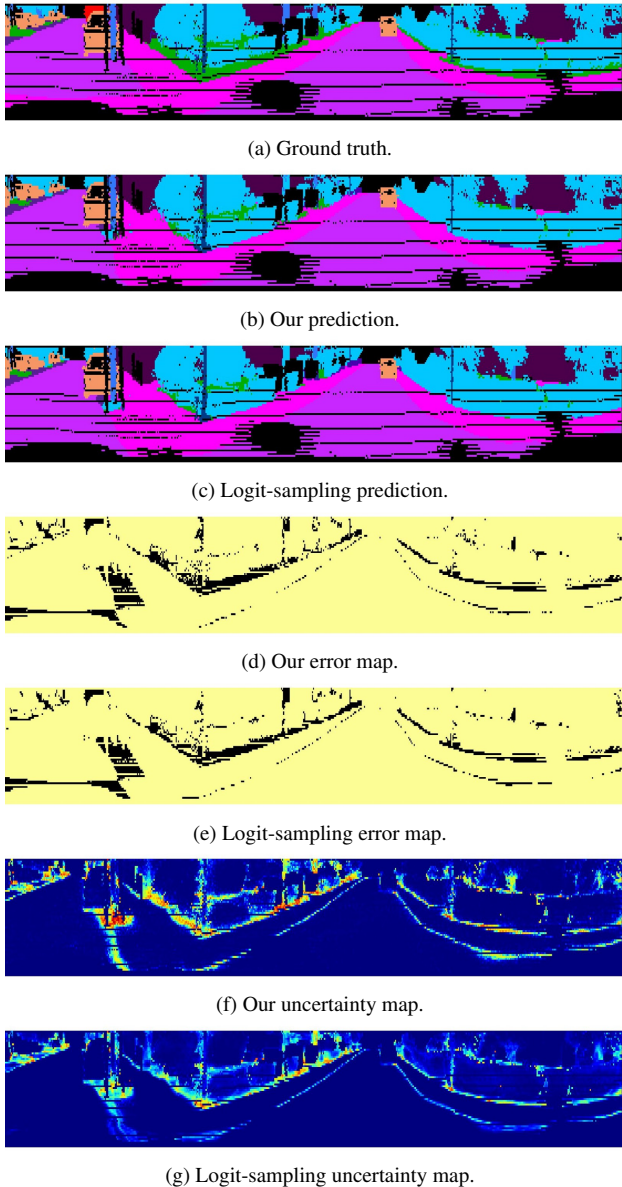


Figure 3. Comparative qualitative visualization of LiDAR semantic scene segmentation and uncertainty analysis. (a) Ground truth for the scene, where colors indicate the classes. (b) Prediction map from our sampling-free approach. (c) Prediction map from logit-sampling approach. (d) Error map from our approach, highlighting misclassifications in black. (e) Error map from the logit-sampling approach. (f) Uncertainty map of our sampling-free approach, with uncertainty visualized from low (blue) to high (red). (g) Uncertainty map of logit-sampling.

5. Conclusion

We have developed a method that calculates how likely it is that the class our model predicts is the correct one, by examining the distributions of all possible class outcomes.

We validated our sampling-free confidence estimation for LiDAR scene semantic segmentation, a field where safety-critical responses and real-time processing for large-scale data are crucial. The comprehensive analysis comparing the lower bound confidence values with exact ones, approximated through Monte Carlo integration, demonstrates a negligible discrepancy, confirming the robustness of the sampling-free lower bound confidence for practical applications. Furthermore, when compared to the sampling approach during inference, the proposed method consistently generates well-calibrated confidence values, exhibiting low ACE and calibrated reliability diagrams. Moreover, our proposed method tends to be slightly underconfident across a broader range of regions while also delivering faster performance. In conclusion, our proposed method effectively performs semantic segmentation of LiDAR scenes, ensuring accurate classification, well-calibrated confidence computation, and real-time performance, while also providing detailed uncertainty maps.

References

- [1] Jens Behley, Martin Garbade, Andres Milioto, Jan Quenzel, Sven Behnke, Cyrill Stachniss, and Jurgen Gall. Semantickitti: A dataset for semantic scene understanding of lidar sequences. In *Proceedings of the IEEE/CVF international conference on computer vision*, pages 9297–9307, 2019. 4
- [2] Tiago Cortinhal, George Tzelepis, and Eren Erdal Aksoy. Salsanext: Fast, uncertainty-aware semantic segmentation of lidar point clouds. In *Advances in Visual Computing: 15th International Symposium, ISVC 2020, San Diego, CA, USA, October 5–7, 2020, Proceedings, Part II 15*, pages 207–222. Springer, 2020. 2, 4, 5
- [3] Yarin Gal and Zoubin Ghahramani. Dropout as a bayesian approximation: Representing model uncertainty in deep learning. In *international conference on machine learning*, pages 1050–1059. PMLR, 2016. 2
- [4] Yarin Gal et al. Uncertainty in deep learning. *thesis, University of Cambridge*, 2016. 1
- [5] Chuan Guo, Geoff Pleiss, Yu Sun, and Kilian Q Weinberger. On calibration of modern neural networks. In *International conference on machine learning*, pages 1321–1330. PMLR, 2017. 1, 2, 4
- [6] Yulan Guo, Hanyun Wang, Qingyong Hu, Hao Liu, Li Liu, and Mohammed Bennamoun. Deep learning for 3d point clouds: A survey. *IEEE transactions on pattern analysis and machine intelligence*, 43(12):4338–4364, 2020. 2
- [7] Jing Huang and Suya You. Point cloud labeling using 3d convolutional neural network. In *2016 23rd International Conference on Pattern Recognition (ICPR)*, pages 2670–2675. IEEE, 2016. 2
- [8] Alex Kendall and Yarin Gal. What uncertainties do we need in bayesian deep learning for computer vision? *Advances in neural information processing systems*, 30, 2017. 1, 2, 3, 5
- [9] Alex Kendall, Vijay Badrinarayanan, and Roberto Cipolla.



(a) Ground truth.



(b) Our prediction.



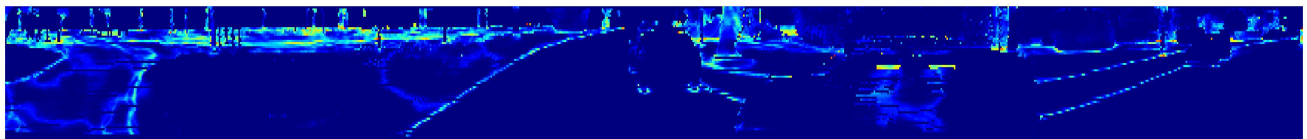
(c) Logit-sampling prediction.



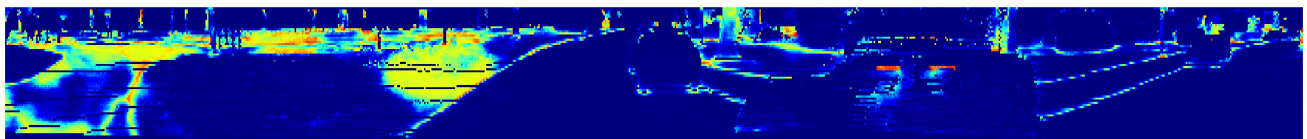
(d) Our error map.



(e) Logit-sampling error map.



(f) Our uncertainty map.



(g) Logit-sampling uncertainty map.

Figure 4. Comparative qualitative visualization of LiDAR semantic scene segmentation and uncertainty analysis. (a) Ground truth for the scene, where colors indicate the classes. (b) Prediction map from our sampling-free approach. (c) Prediction map from logit-sampling approach. (d) Error map from our approach, highlighting misclassifications in black. (e) Error map from the logit-sampling approach. (f) Uncertainty map of our sampling-free approach, with uncertainty visualized from low (blue) to high (red). (g) Uncertainty map of logit-sampling.

Bayesian segnet: Model uncertainty in deep convolutional encoder-decoder architectures for scene understanding. *arXiv preprint arXiv:1511.02680*, 2015. 1, 2

Telmo Silva Filho, Hao Song, and Peter Flach. Beyond temperature scaling: Obtaining well-calibrated multi-class probabilities with dirichlet calibration. *Advances in neural information processing systems*, 32, 2019. 2

[10] Meelis Kull, Miquel Perello Nieto, Markus Kängsepp,

- [11] Balaji Lakshminarayanan, Alexander Pritzel, and Charles Blundell. Simple and scalable predictive uncertainty estimation using deep ensembles. *Advances in neural information processing systems*, 30, 2017. [1](#), [2](#), [5](#)
- [12] Kimin Lee, Honglak Lee, Kibok Lee, and Jinwoo Shin. Training confidence-calibrated classifiers for detecting out-of-distribution samples. *arXiv preprint arXiv:1711.09325*, 2017. [2](#)
- [13] Jishnu Mukhoti, Andreas Kirsch, Joost van Amersfoort, Philip HS Torr, and Yarin Gal. Deep deterministic uncertainty: A new simple baseline. In *Proceedings of the IEEE/CVF Conference on Computer Vision and Pattern Recognition*, pages 24384–24394, 2023. [3](#)
- [14] Mahdi Pakdaman Naeini, Gregory Cooper, and Milos Hauskrecht. Obtaining well calibrated probabilities using bayesian binning. In *Proceedings of the AAAI conference on artificial intelligence*, 2015. [4](#)
- [15] Radford M Neal. *Bayesian learning for neural networks*. Springer Science & Business Media, 2012. [1](#), [2](#)
- [16] Jeremy Nixon, Michael W Dusenberry, Linchuan Zhang, Ghassen Jerfel, and Dustin Tran. Measuring calibration in deep learning. In *CVPR workshops*, 2019. [2](#), [4](#)
- [17] Charles Ruizhongtai Qi, Li Yi, Hao Su, and Leonidas J Guibas. Pointnet++: Deep hierarchical feature learning on point sets in a metric space. *Advances in neural information processing systems*, 30, 2017. [2](#)
- [18] Murat Sensoy, Lance Kaplan, and Melih Kandemir. Evidential deep learning to quantify classification uncertainty. *Advances in neural information processing systems*, 31, 2018. [2](#), [5](#)
- [19] Chenfeng Xu, Bichen Wu, Zining Wang, Wei Zhan, Peter Vajda, Kurt Keutzer, and Masayoshi Tomizuka. Squeeze-seg3: Spatially-adaptive convolution for efficient point-cloud segmentation. In *Computer Vision–ECCV 2020: 16th European Conference, Glasgow, UK, August 23–28, 2020, Proceedings, Part XXVIII 16*, pages 1–19. Springer, 2020. [2](#)
- [20] Bianca Zadrozny and Charles Elkan. Transforming classifier scores into accurate multiclass probability estimates. In *Proceedings of the eighth ACM SIGKDD international conference on Knowledge discovery and data mining*, pages 694–699, 2002. [2](#)